# Apparent Diffusion Coefficient in Pancreatic Cancer: Characterization and Histopathological Correlations

Original Research

# Apparent Diffusion Coefficient in Pancreatic Cancer: Characterization and Histopathological Correlations

**Noriaki Muraoka, M.D.[1]; Hidemasa Uematsu, M.D., Ph.D.[1];**

**Hirohiko Kimura, M.D., Ph.D.[1]; Yoshiaki Imamura, M.D., Ph.D.[2];**

**Yasuhiro Fujiwara, R.T.[1]; Makoto Murakami, M.D., Ph.D.[3];**

**Akio Yamaguchi, M.D., Ph.D. [3]; Harumi Itoh, M.D., Ph.D.[1]**

Departments of [1]Radiology, [2]Pathology and [3]First Department of Surgery,

University of Fukui

Correspondence should be addressed to **Noriaki Muraoka, M.D.**

Department of Radiology, University of Fukui,

23 Matsuoka-shimoaizuki, Eiheiji-cho, Yoshida-gun, Fukui 910-1193, Japan

Phone: +81-776-61-8371; Fax: +81-776-61-8137

E-mail: nmuraoka@u-fukui.ac.jp

Running title: ADC value in pancreatic cancer

**ABSTRACT** (171 words)

**Purpose:** To clarify the components primarily responsible for diffusion abnormalities in pancreatic cancerous tissue.

**Materials and Methods:** Subjects comprised 10 patients with surgically confirmed pancreatic cancer. Diffusion-weighted (DW) echo-planar imaging (b value=0, 500 s/mm$^2$) was employed to calculate ADC. ADC values of cancer and non-cancerous tissue were calculated. Furthermore, ADC values of the cancer were compared with histopathological results.

**Results:** Mean (±standard deviation) ADC value was significantly lower for tumor (1.27±0.52 ×10$^{-3}$ mm$^2$/s) than for non-cancerous tissue (1.90±0.41×10$^{-3}$ mm$^2$/s, P<0.05). Histopathological examination showed similar proportions of fibrotic area, cellular component, necrosis and mucin in each case. Regarding the density of fibrosis in cancer, 3 cases were classified to the loose fibrosis group, and the remaining 7 cases were classified to the dense fibrosis group. Mean ADC value was significantly higher in the loose fibrosis group (1.88±0.39×10$^{-3}$ mm$^2$/s) than in the dense fibrosis group (1.01±0.29×10$^{-3}$ mm$^2$/s, P<0.05). In quantitative analysis, ADC correlated well with proportion of collagenous fibers (r=-0.87, P<0.05).

**Conclusion:** Collagenous fibers may be responsible for diffusion abnormalities in pancreatic cancer.

**Key Words:** pancreatic cancer; diffusion-weighted imaging; apparent diffusion coefficient;

histopathological correlations

## INTRODUCTION

Pancreatic ductal adenocarcinoma is a serious disease with poor prognosis. Diagnosis

at an early stage, when the tumor is small and localized, is thus crucial for potential cure with

surgery. Unfortunately, pancreatic ductal adenocarcinoma is usually diagnosed in the late

stages, due to nonspecific clinical signs and symptoms (1). Ultrasonography, computed

tomography (CT), magnetic resonance imaging (MRI) and endoscopic retrograde

cholangiography are the most frequent diagnostic methods used for evaluating patients with

clinically suspected pancreatic cancer (2-4). However, these methods have difficulty in

distinguishing pancreatic cancer from other pancreatic lesions, and in differentiating tumor

lesions from normal pancreas (5).

Diffusion-weighted imaging (DWI) has recently seen extensive use in the central

nervous system (CNS) for imaging of tumors (6, 7) and acute stroke (8). Various technical

advances have allowed DWI and measurement of apparent diffusion coefficient (ADC) for the

abdominal region (9-12). Ichikawa et al. (13) reported that high b-value DWI might be a

useful tool for detecting pancreatic adenocarcinoma with high sensitivity and specificity.

Yoshikawa et al. (12) reported that pancreatic cancer had an ADC value higher than that of

normal pancreas, although the study included a small number of patients. To the best of our

knowledge, pathological correlations with ADC values have not been reported for pancreatic

carcinoma.

Demachi et al. (14) reported correlations between dynamic CT findings and the

histopathological features of pancreatic ductal adenocarcinoma, and concluded that the degree

of contrast enhancement is related to histological features such as dense fibrosis, increasing

cellularity, acinar tissue and mucin. Itoh et al. (15) reported that pancreatic carcinoma displays

either loose fibrosis or dense fibrosis, and the histopathological features might affect tumor

enhancement in early-phase contrast-enhanced CT. We therefore hypothesized that these

histopathological variations might influence ADC values of the tumor. Our purpose was to

clarify the components primarily responsible for diffusion abnormalities in pancreatic

cancerous tissue.

**MATERIALS AND METHODS**

The initial subject population comprised 35 patients with pancreatic cancer (24 men,

11 women; mean age, 67.2 years; range, 47-85 years) recruited between January 2005 and

June 2007. We finally selected 10 subjects (7 men, 3 women; mean age, 67.7 years; range,

57-74 years) with surgically confirmed pancreatic cancer for evaluation of pathological

correlations to ADC value. Mean maximum lesion diameter was 26.1 mm (range, 11-51 mm)

and lesions were located in the head (n=2), body (n=4), tail (n=1) or uncus (n=3) of the

pancreas. All study protocols were approved by our institutional review board, and informed

consent was obtained from all patients before enrollment in this study.

**MRI**

All MRI examinations were performed on a clinical 1.5-T scanner (Signa Excite; GE

Healthcare, Milwaukee, WI) in combination with an 8-channel phased-array coil (USA

Instruments, Aurora, OH). Initial imaging consisted of axial T2-weighted fast spin-echo

imaging (T2-WI) with fat suppression (repetition time (TR), 2100 ms; echo time (TE), 89.2

ms; echo train length, 17 times; field-of view (FOV), 34.0 cm; slice thickness, 4.0 mm; space,

1.0 mm; phase FOV, 1.00; asset factor, 2; number of excitations (NEX), 2; matrix, 256×224),

T1-weighted dynamic contrast-enhanced imaging (T1-WI) with fat suppression (fast spoiled

gradient echo recalled acquisition in the steady state; TR, 210 ms; TE, 1.7 ms; FOV, 34.0 cm;

flip angle, 80°; bandwidth, 31.25 kHz; asset factor, 2; NEX, 1.0; matrix: 288×192) and

magnetic resonance cholangiopancreatography (3D fast recovery fast spin echo respiratory

triggering; TR, 3300-7800 ms; effective TE, 643 (variable) ms; FOV, 36.0 cm; slice thickness,

1.6 mm; asset factor, 2; NEX, 1; matrix, 320×224), focusing on the pancreas to facilitate

disease staging. Following the initial 4 sequences outlined above, DWI was acquired through

the pancreas at 20 slice locations utilizing a finger pulse-triggered diffusion-weighted

single-shot spin-echo echo-planar imaging (EPI) technique (TR, time between R-peaks (R-R)

$\times$7 ms; TE, 63.5 ms; b=0 and 500 s/mm$^2$, RR interval, 7; trigger window, 20%; trigger delay,

minimum; inter-sequence delay, minimum; cardiac phases single FOV, 34.0 cm; slice

thickness, 5 mm; spacing, 1 mm; asset factor, 2; NEX, 8; matrix, 128$\times$128). All axial images

were reconstructed to 256$\times$256 matrix images after scanning.

**Analysis of DWI**

DWI was analyzed using free image analysis software (Image J version 1.33;

http://rsb.info.nih.gov/ij/) on Windows to calculate ADC values of the tumor and

non-cancerous tissue. All regions of interest (ROIs) were placed by the consensus decision of

two radiologists (N.M., H.U.), with reference to other sequences such as T1-WI and T2-WI.

ROIs were placed in tumor and non-cancerous tissue as large as possible. Areas of ROIs were

between 59.9 mm$^2$and 246.9 mm$^2$ (mean, 117.2 mm$^2$; median, 100 mm$^2$) and pixel counts of

ROIs were between 34 and 140 pixels (1 pixel: 1.76 mm$^2$).

When ROIs were drawn, great care was taken to exclude both the dilated pancreatic duct and

cystic lesion including retention cyst and pseudocyst to reduce any error in precise ADC

calculations. When the b value was 500 s/mm$^2$, ADC value (D) was calculated according to

the following formula (16):

$$\ln[S(500)/S(0)] = -b \cdot D$$

**Histological analysis**

Resected tumor specimens were fixed in formalin, then stained using hematoxylin and eosin (HE) for diagnosis. By referring to DWI and photographs of the gross specimen, a pathologist (Y. I., with 20 years of experience) and a radiologist (N.M., with 13 years of experience) determined the sections of each tumor that corresponded to the DWI slice plane by consensus. Each area proportion of histological findings of pancreatic cancer such as fibrosis, cellular component, necrosis and mucin were visually rated in 4 grades (Grades 1-4) in each case. Grades of each pathological feature occupying the whole specimen were defined as follows: Grade 1, 0-15%; Grade 2, 15-30%; Grade 3, 30-45%; and Grade 4, 45-60%. Furthermore, patients were classified into two groups: a loose fibrosis group; and a dense fibrosis group (15). Grades and classifications in each case were again decided by the consensus decision of two authors (N.M., Y.I.).

Specimens were also stained with trichrome to dye collagen fibers blue for quantitative evaluation of fibrosis in pancreatic cancer. For quantitative evaluation, the proportion of collagenous fiber was determined in 10 views (histological fields ×40) corresponding to the tumor ROI on DWI. Image analysis software (Mac Scope version 2.56; Mitani, Fukui, Japan) on a Macintosh computer was used for this evaluation. Selection of

these 10 visual fields was determined by the consensus decision of two authors (N.M., Y.I.).

**Statistical analysis**

ADC values were compared between tumor and non-cancerous tissue using the Wilcoxon matched-pairs test. In addition, ADC values were compared between the loose fibrosis group and dense fibrosis group using the Mann-Whitney test. Relationships between ADC value of tumor and proportion of collagenous fiber were analyzed by simple regression with Pearson's correlation coefficient. Values of P<0.05 were considered statistically significant.

**RESULTS**

Patient profiles are summarized in Table 1. Mean (±standard deviation) ADC value was significantly lower for the tumor ($1.27\pm0.52 \times10^{-3}$ mm$^2$/s) than for non-cancerous tissue ($1.90\pm0.41\times10^{-3}$ mm$^2$/s, P<0.05) (Fig.1). Regarding the density of fibrosis, 3 cases were classified to the loose fibrosis group, and the remaining 7 cases were classified to the dense fibrosis group. As shown in Figure 2, mean ADC value was significantly higher for the loose fibrosis group (n=3; $1.88\pm0.39\times10^{-3}$ mm$^2$/s) than for the dense fibrosis group (n=7; $1.01\pm0.29\times10^{-3}$ mm$^2$/s, P<0.05). Representative cases are shown in Figures 3 and 4.

Under 4-step visual evaluation (Table 2), mucin and necrosis were judged as grade 1

(<15%) in all cases. Concerning cellular components, 1 case was judged as grade 4, but the

remaining 9 cases were judged as grade 3. Concerning fibrosis, 2 cases were judged as grade

3, but the remaining 8 cases were judged as grade 4.

In the loose fibrosis group, histopathological examination showed that edematous

fibrosis and loose collagen fibers were more prevalent than cellular component or mucin (Fig.

3C, D). In the dense fibrosis group, dense collagenous fibers were dominant compared with

cellular component, coagulative necrosis and mucin (Fig. 4C, D), and pathological features

differed completely from those in the loose fibrosis group. A significant correlation was

identified between ADC values and mean proportion of collagenous fibers (r=-0.87, P<0.05)

(Fig. 5).

## DISCUSSION

In this study, mean ADC value was significantly lower for the tumor than for

non-cancerous tissue. However both ADC values varied widely and a large overlap was

apparent. Histopathological examination demonstrated similar areas of fibrosis, cellular

component, necrosis and mucin, but density of fibrosis varied widely between cases. With

regard to the density of fibrosis, 3 cases were classified to the loose fibrosis group, and the

remaining 7 cases were classified to the dense fibrosis group. ADC values were significantly

higher for the loose fibrosis group than for the dense fibrosis group. Furthermore, quantitative

analysis revealed that ADC correlated well with the proportion of collagenous fibers.

Several authors have reported imaging findings in relation to histological features of

pancreatic carcinoma (14, 15, 17, 18). Cellular component represents one of the

histopathological features that could correlate with ADC value. Sugahara et al. (6) reported

that minimum ADC value correlates well with histological cellularity in gliomas. Guo et al.

(7) also reported a clear inverse relationship between ADC value and cellular component of

brain tumors, such as lymphoma and high-grade astrocytoma. ADC value was significantly

lower in lymphomas than in high-grade gliomas, while cellular component was significantly

greater in lymphomas than in high-grade gliomas. Those findings suggest that increased

cellularity is associated with more restricted diffusion. In the present study, visual grading of

the cellular component was grade 3 for 9 cases and grade 4 for 1 case, while density of the

cellular component in each case was the same. We thus considered the cellular component as

one cause of restricted diffusion. However, no major differences in grade or density of the

cellular component were seen between the present cases, so the influence of cellular

component on ADC values was difficult to discern in this study.

Necrosis is also one of the pathological features in pancreatic cancer, and might be

associated with increasing diffusion. Lyng et al. (19) reported that the fraction of massive

necrosis could correlate with ADC values, but not the fraction of small necrotic foci, as the

size of such foci may be smaller than voxels on MRI. In the present study, degree of necrosis

was grade 1 in all cases, representing a small factor in pathological features. Necrosis was

thus considered to display no correlation with ADC value.

Mucin may be associated with more restricted diffusion compared with other fluids similar to water. Yamashita et al. (20) reported that DWI can help differentiate mucin-producing tumor (MPT) of the pancreas from other cystic lesions, as viscous fluid within MPT displays restricted water diffusion. However, the presence of mucin in our study was judged to be grade 1 and showed the same degree in all cases. We considered that mucin within a solid tumor would probably show increased diffusion compared with other solid components. Mucin was thus considered one factor affecting ADC values, but not the main cause for restriction of water diffusion in pancreatic cancer.

Fibrosis (desmoplasia) is the most characteristic feature of pancreatic cancer, and might be associated with restricted diffusion. Bachem et al. (21) reported that pancreatic carcinoma cells induce fibrosis by stimulating proliferation and matrix synthesis of stellate cells, which strongly support tumor growth and result in increased deposition of connective tissue. Previous research has reported that increasing development of fibrous connective tissue in the liver would decrease ADC values and might decrease water content histologically (22-26). In this study, ADC values were significantly higher in the loose fibrosis group than in the dense fibrosis group in cancerous areas. Furthermore, a significant correlation was identified between ADC values and mean proportion of collagenous fibers. For example, between Case 5 and Case 6, visual grading of fibrotic area was the same (grade 4), but density

of fibrosis differed and the proportions of collagenous fibers were 9.3% and 52.8%,

respectively. In the loose fibrosis group, histological examination showed edematous fibrosis

and loose collagen fibers as pathological features and ADC values were higher in the

cancerous area. This result was consistent with the findings of a previous study (12).

Conversely, the dense fibrosis group exhibited lower ADC values in the cancerous area. We

thus considered that increases in collagenous fibers are generally seen in pancreatic cancer

and fibrosis can be present as dense fibrosis or edematous fibrosis, with differing

histopathological findings associated with various ADC values for pancreatic cancer.

In this study, tumors with a similar degree of fibrosis of around 50% still showed

large variations in ADC for the 7 patients who showed lower ADC in the tumor compared to

the non-cancerous pancreas (Fig. 5). Visual grading of each pathological component was

nearly equal in each case (Table 2). Variations in ADC value for the 7 patients who showed

lower ADC in the tumor compared to non-cancerous pancreas thus could not be clearly

explained by visual grading alone. As each visual grade has a range of 15% in each grade, the

summation of ranges for the 4 components may be responsible for variation in ADC values

for the 7 patients.

Measurement of ADC value was not clinically useful for detecting pancreatic

carcinoma, including tumor extent, as ADC values vary and overlap between cancer and

non-cancerous tissues. However, ADC values in cancer tissue might be affected by

differences in histopathological features. In particular, density of fibrosis might be one of the

major causes of variable ADC values. Clarification of correlations between histopathological

features and ADC values might lead to improved evaluation of the prognosis and efficacy of

treatment for pancreatic cancers in future.

The present study displays some limitations. First, the number of surgically resected

subjects was limited, as many cases were inoperative due to advanced pancreatic cancer.

Second, regarding the amount of fibrosis, we performed quantitative evaluation of

the proportion of fibrosis. However, cellular components such as necrosis and mucin that

form other major pathological features were only visual evaluated from grade 1 to grade 4.

Quantitative evaluation of these histological features using specific stainings is also warranted

to clarify whether these histological features area can cause variations in ADC value.

Third, although we calculated ADC values in tumor and non-cancerous tissues and

compared these values between tumor and non-cancerous tissues, ADC values of

non-cancerous tissues varied widely (1.35-2.57). Actually, non-cancerous tissues might be

affected by diffuse fibrosis due to chronic pancreatitis, active inflammation, pancreatic duct

dilatation or pseudocysts due to acute pancreatitis. Such findings are commonly seen as

secondary changes in patients with pancreatic carcinoma (27). Assessment of fibrosis in the

non-cancerous pancreas should thus be added. However, pathological assessment of the

non-cancerous tissues was impossible, as insufficient non-cancerous specimens were obtained.

Ideally, calculation of mean ADC values for normal pancreatic tissue from normal volunteers and comparison between ADC values for tumors and mean values of normal pancreatic tissue would be performed.

Fourth, regarding the histopathological examination, we visually evaluated intratumoral mucin to determine the grading using only HE staining. However, additional intratumoral mucin would be present that was not visualized without specific stains, such as Periodic Acid Schiff reaction or Alcian Blue stain. The true amount of mucin might thus be greater than the quantity of mucin identified in this study.

Fifth, imaging investigations were performed using a relatively low b value (b=500 s/mm$^2$), to minimize motion artifacts and improve signal-to-noise ratio in abdominal organs. However, the use of higher b values is more desirable to reflect true diffusion. Only two b values (500 and 0 s/mm$^2$) were used to measure ADC values, due to limitations on inspection time in the clinical setting. Ideally, multiple b values should be set up for exact measurement of ADC values.

Finally, echo-planar DWI is limited by notable susceptibility artifacts in the abdomen, due to abdominal wall motion and adjacent bowel gas. DWI techniques that are insensitive to susceptibility artifacts are thus necessary for the evaluation of abdominal lesions. We used a finger pulse-triggered diffusion-weighted single-shot spin-echo EPI technique with parallel imaging to reduce motion and susceptibility artifacts. As line-scan DWI is inherently

insensitive to susceptibility artifacts (28), clinical application of line-scan DWI to abdominal

lesions may be desirable.

In conclusion, ADC correlates well with proportion of collagenous fibers, which may

thus be responsible for diffusion abnormalities in pancreatic cancer.

**REFERENCES**

1.      Warshaw AL, Fernandez-del Castillo C. Pancreatic carcinoma. N Engl J Med 1992;

        326:455-465.

2.      Freeny PC, Marks WM, Ryan JA, et al. Pancreatic ductal adenocarcinoma: diagnosis

        and staging with dynamic CT. Radiology 1988; 166:125-133.

3.      O'Malley ME, Boland GW, Wood BJ, et al. Adenocarcinoma of the head of the

        pancreas: determination of surgical unresectability with thin-section pancreatic-phase

        helical CT. AJR Am J Roentgenol 1999; 173:1513-1518.

4.      Gabata T, Matsui O, Kadoya M, et al. Small pancreatic adenocarcinomas: efficacy of

        MR imaging with fat suppression and gadolinium enhancement. Radiology 1994;

        193:683-688.

5.      Johnson PT, Outwater EK. Pancreatic carcinoma versus chronic pancreatitis: dynamic

        MR imaging. Radiology 1999; 212:213-218.

6.      Sugahara T, Korogi Y, Kochi M, et al. Usefulness of diffusion-weighted MRI with

        echo-planar technique in the evaluation of cellularity in gliomas. J Magn Reson

        Imaging 1999; 9:53-60.

7.      Guo AC, Cummings TJ, Dash RC, et al. Lymphomas and high-grade astrocytomas:

        comparison of water diffusibility and histologic characteristics. Radiology 2002;

        224:177-183.

8.    Warach S, Chien D, Li W, et al. Fast magnetic resonance diffusion-weighted imaging of acute human stroke. Neurology 1992; 42:1717-1723.

9.    Ichikawa T, Haradome H, Hachiya J, et al. Diffusion-weighted MR imaging with single-shot echo-planar imaging in the upper abdomen: preliminary clinical experience in 61 patients. Abdom Imaging 1999; 24:456-461.

10.    Murtz P, Flacke S, Traber F, et al. Abdomen: diffusion-weighted MR imaging with pulse-triggered single-shot sequences. Radiology 2002; 224:258-264.

11.    Chow LC, Bammer R, Moseley ME, et al. Single breath-hold diffusion-weighted imaging of the abdomen. J Magn Reson Imaging 2003; 18:377-382.

12.    Yoshikawa T, Kawamitsu H, Mitchell DG, et al. ADC measurement of abdominal organs and lesions using parallel imaging technique. AJR Am J Roentgenol 2006; 187:1521-1530.

13.    Ichikawa T, Erturk SM, Motosugi U, et al. High-b value diffusion-weighted MRI for detecting pancreatic adenocarcinoma: preliminary results. AJR Am J Roentgenol 2007; 188:409-414.

14.    Demachi H, Matsui O, Kobayashi S, et al. Histological influence on contrast-enhanced CT of pancreatic ductal adenocarcinoma. J Comput Assist Tomogr 1997; 21:980-985.

15.    Itoh S, Satake H, Ohta T, et al. Pancreatic ductal adenocarcinoma showing iso-attenuation in early-phase contrast-enhanced CT: comparison with

histopathological findings. Radiat Med 2002; 20:59-67.

16. Burdette JH, Elster AD, Ricci PE. Calculation of apparent diffusion coefficients (ADCs) in brain using two-point and six-point methods. J Comput Assist Tomogr 1998; 22:792-794.

17. Bluemke DA, Cameron JL, Hruban RH, et al. Potentially resectable pancreatic adenocarcinoma: spiral CT assessment with surgical and pathologic correlation. Radiology 1995; 197:381-385.

18. Ichikawa T, Haradome H, Hachiya J, et al. Pancreatic ductal adenocarcinoma: preoperative assessment with helical CT versus dynamic MR imaging. Radiology 1997; 202:655-662.

19. Lyng H, Haraldseth O, Rofstad EK. Measurement of cell density and necrotic fraction in human melanoma xenografts by diffusion weighted magnetic resonance imaging. Magn Reson Med 2000; 43:828-836.

20. Yamashita Y, Namimoto T, Mitsuzaki K, et al. Mucin-producing tumor of the pancreas: diagnostic value of diffusion-weighted echo-planar MR imaging. Radiology 1998; 208:605-609.

21. Bachem MG, Schunemann M, Ramadani M, et al. Pancreatic carcinoma cells induce fibrosis by stimulating proliferation and matrix synthesis of stellate cells. Gastroenterology 2005; 128:907-921.

22. Koinuma M, Ohashi I, Hanafusa K, et al. Apparent diffusion coefficient measurements with diffusion-weighted magnetic resonance imaging for evaluation of hepatic fibrosis. J Magn Reson Imaging 2005; 22:80-85.

23. Boulanger Y, Amara M, Lepanto L, et al. Diffusion-weighted MR imaging of the liver of hepatitis C patients. NMR Biomed 2003; 16:132-136.

24. Namimoto T, Yamashita Y, Sumi S, et al. Focal liver masses: characterization with diffusion-weighted echo-planar MR imaging. Radiology 1997; 204:739-744.

25. Yamada I, Aung W, Himeno Y, et al. Diffusion coefficients in abdominal organs and hepatic lesions: evaluation with intravoxel incoherent motion echo-planar MR imaging. Radiology 1999; 210:617-623.

26. Chan JH, Tsui EY, Luk SH, et al. Diffusion-weighted MR imaging of the liver: distinguishing hepatic abscess from cystic or necrotic tumor. Abdom Imaging 2001; 26:161-165.

27. Muller MF, Meyenberger C, Bertschinger P, et al. Pancreatic tumors: evaluation with endoscopic US, CT, and MR imaging. Radiology 1994; 190:745-751.

28. Maeda M, Kato H, Sakuma H, et al. Usefulness of the apparent diffusion coefficient in line scan diffusion-weighted imaging for distinguishing between squamous cell carcinomas and malignant lymphomas of the head and neck. AJNR Am J Neuroradiol 2005; 26:1186-1192.

**TABLES**

Table 1: Summary of patients with pancreatic cancer

| Case | Age/sex | Location | Tumor Size (mm) | ADC value (tumor) $\times 10^{-3}$ mm$^2$/s | ADC (non-cancerous tissue) |
|---|---|---|---|---|---|
| 1 | 64F | uncus | 30 | 1.15±0.31 | 2.57±0.42 |
| 2 | 70F | uncus | 21 | 0.42±0.17 | 2.05±0.46 |
| 3 | 57M | body | 11 | 1.28±0.19 | 2.51±0.20 |
| 4 | 77M | tail | 51 | 1.18±0.17 | 1.93±0.50 |
| 5 | 71M | body | 11 | 2.32±0.22 | 1.7±0.23 |
| 6 | 73M | body | 22 | 1.12±0.16 | 2.09±0.41 |
| 7 | 68M | head | 25 | 1.76±0.16 | 1.52±0.29 |
| 8 | 68M | body | 30 | 1.04±0.14 | 1.79±0.23 |
| 9 | 74F | head | 22 | 1.57±0.21 | 1.53±0.19 |
| 10 | 55M | uncus | 38 | 0.89±0.13 | 1.35±0.12 |

Table 2: Visual grading of tumor components

| Case | Fibrosis | Necrosis | Cellularity | Mucin |
|------|----------|----------|-------------|-------|
| 1 | 4 (dense) | 1 | 3 | 1 |
| 2 | 3 (dense) | 1 | 3 | 1 |
| 3 | 4 (dense) | 1 | 3 | 1 |
| 4 | 4 (dense) | 1 | 3 | 1 |
| 5 | 4 (loose) | 1 | 3 | 1 |
| 6 | 4 (dense) | 1 | 4 | 1 |
| 7 | 4 (loose) | 1 | 3 | 1 |
| 8 | 3 (dense) | 1 | 3 | 1 |
| 9 | 4 (loose) | 1 | 3 | 1 |
| 10 | 4 (dense) | 1 | 3 | 1 |

The 4 grades of each pathological feature occupying the specimen were defined as: Grade 1, 0-15%; Grade 2, 15-30%; Grade 3, 30-45%; Grade 4, 45-60%. Fibrosis was classified by the density of collagen fiber as loose or dense.

**FIGURE LEGENDS**
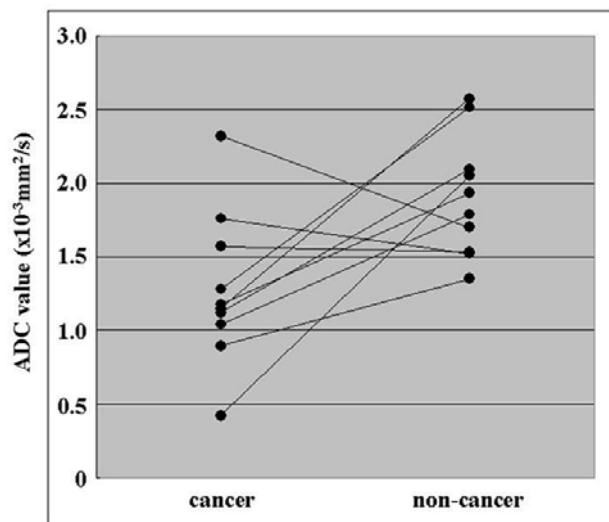


**Figure 1: Summary of ADC values in patients with pancreatic cancer (n=10)**

Mean (±standard deviation) ADC value was significantly lower in tumor ($1.27 \pm 0.52 \times 10^{-3}$ $mm^2$/s) than in non-cancerous tissue ($1.90 \pm 0.41 \times 10^{-3}$ $mm^2$/s, $P<0.05$).
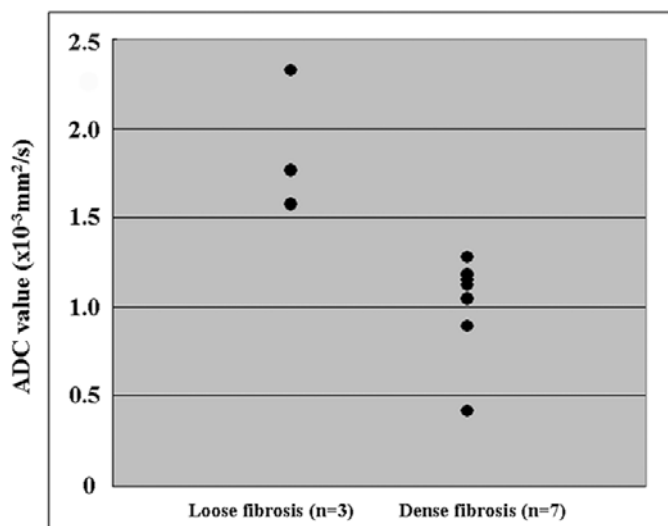


**Figure 2: Scatter plots of ADC values in the loose fibrosis group (n=3) and dense fibrosis group (n=7)**

Mean ADC value was significantly higher in the loose fibrosis group ($1.88 \pm 0.39 \times 10^{-3}$ $mm^2$/s)

than in the dense fibrosis group ($1.01\pm0.29\times10^{-3}$ mm$^2$/s, P<0.05). No overlap between groups was apparent.
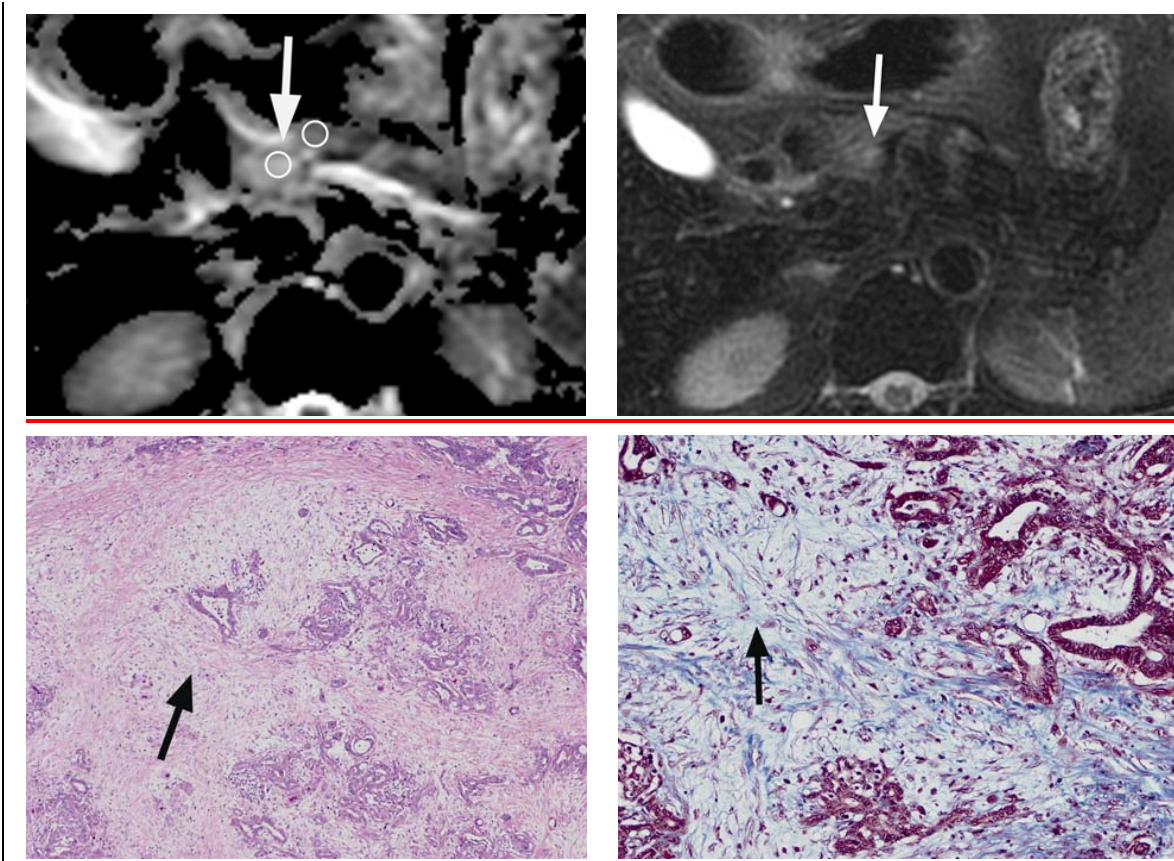


**Figure 3: A 71-year-old man with well-differentiated ductal adenocarcinoma of the pancreas head**

**A)** ADC mapping demonstrates the tumor (white arrow) as a signal hyperintense lesion, and ADC values for the tumor and non-cancerous tissue were $2.32\times10^{-3}$ mm$^2$/s and $1.70\times10^{-3}$ mm$^2$/s, respectively. ROIs were placed in the tumor and non-cancerous tissue as large as possible. **B)** Corresponding respiratory-triggered T2-weighted MRI shows the tumor as a signal hyperintense lesion (white arrow). **C)** Edematous collagenous fibers (black arrow) were found in this pancreatic cancer (HE; original magnification ×10). **D)** Edematous collagenous

fibers (black arrow) were stained by trichrome, dyeing blue. The proportion of collagenous

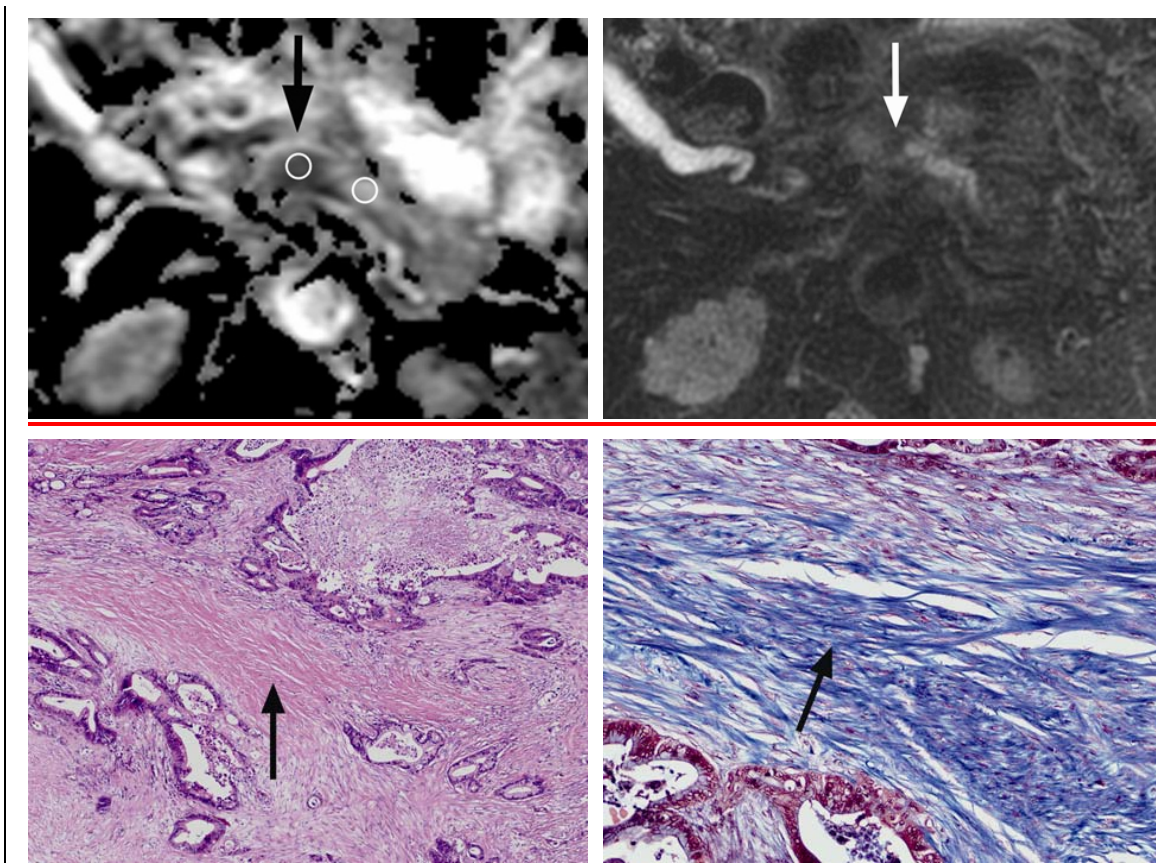fiber occupying visual fields was 9.3% (original magnification ×40).



**Figure 4: A 73-year-old man with well-differentiated ductal adenocarcinoma in the body**

**of the pancreas**

**A)** ADC values of this tumor (black arrow) and non-cancerous tissue were $1.12\times10^{-3}$ mm$^2$/s

and $2.09\times10^{-3}$ mm$^2$/s, respectively. ROIs were placed in the tumor and non-cancerous tissue

as large as possible. **B)** Corresponding respiratory-triggered T2-weighted MR image shows

the tumor as the low signal lesion (white arrow). **C)** Dense collagenous fiber (black arrow)

was found in this pancreatic cancer (HE, original magnification×10). **D)** Dense collagenous

fibers (black arrow) were stained blue by trichrome dyeing. The proportion of collagenous

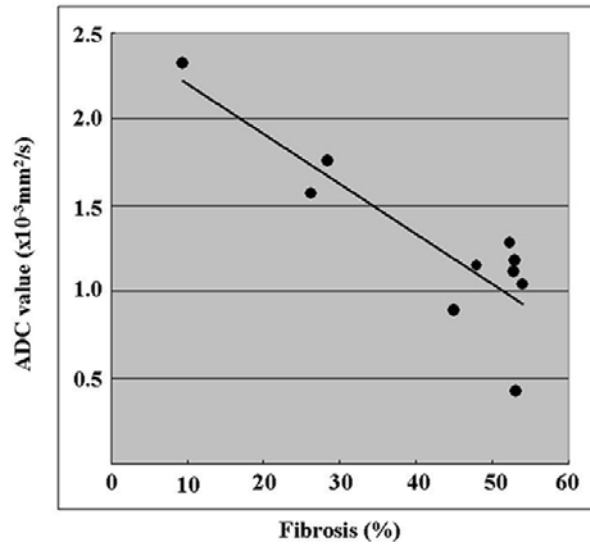fibers occupying visual fields was 52.8% (original magnification×40).



**Figure 5: Scatter plot of ADC value of tumor versus proportion of collagenous fiber**

A significant correlation was identified between ADC value and proportion of collagenous

fibers (r=-0.87, p<0.05).